



Enforcing Energy Preservation in Microfacet Models

Davide Sforza¹  and Fabio Pellacini¹ 

¹Sapienza University of Rome, Italy

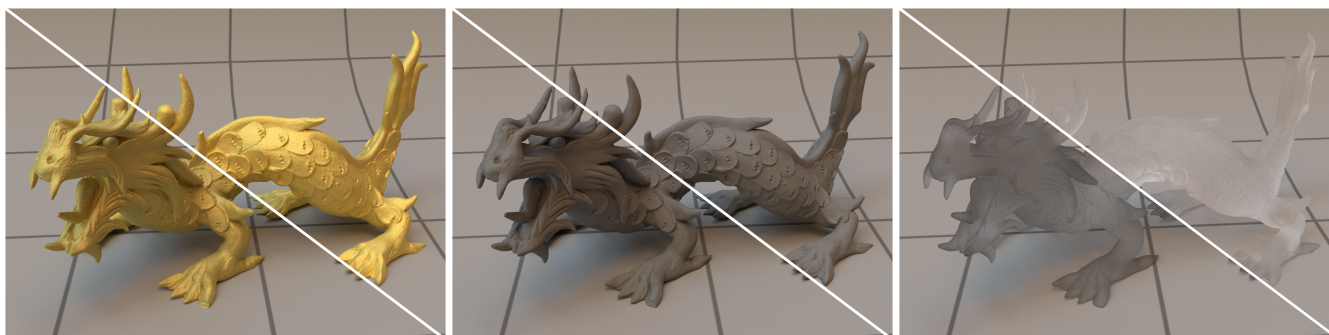


Figure 1: Microfacet models tend to lose energy with the increase in surface roughness, causing an undesired darkening of rough materials. Our method allows compensating for the loss of energy without the use of precomputed look-up tables. Instead, we propose a set of analytic approximations of the directional albedo of conductive (left), glossy (center) and dielectric (right) materials.

Abstract

Microfacet models suffer from a significant limitation: they only simulate a single interaction between light and surface, ignoring the subsequent scattering across the microfacets. As a consequence, the BSDF is not energy preserving, resulting in an unexpected darkening of rough specular surfaces. Energy compensation methods face this limitation by adding to the BSDF a secondary component accounting for multiple scattering contributions. While these methods are fast, robust and can be added to a renderer with relatively minor modifications, they involve the computation of the directional albedo. This quantity is expressed as an integral that does not have a closed-form solution, but it needs to be precomputed and stored in tables. These look-up tables are notoriously cumbersome to use, in particular on GPUs. This work obviates the need of look-up tables by fitting an analytic approximation of the directional albedo, which is a more practical solution. We propose a 2D rational polynomial of degree three to fit conductors and a 3D rational polynomial of degree three to fit dielectrics and materials composed of a specular layer on top of a diffuse one, such as plastics. We enforce energy preservation by rescaling the specular albedo, thus maintaining the same lobe shape. We validated our results via the furnace test, highlighting that materials rendered using our analytic approximations match almost exactly the behaviour of the ones rendered with the use of look-up tables, resulting in an energy-preserving model even at maximum roughness. The software we use to fit coefficients is open-source and can be used to fit other BSDF models as well.

CCS Concepts

• **Computing methodologies** → Reflectance modeling;

1. Introduction

Microfacet models have been introduced for the first time by Torrance and Sparrow [TS67]. These models assume that surfaces that are not perfectly smooth are composed of many tiny facets, each of which is a perfect mirror. Each microfacet is so small that the

surface cannot be represented in a geometric way. Instead, they are modeled in a statistical manner.

Nowadays, microfacet models are considered the industry standard to simulate rough material surfaces, both in real-time and offline rendering. Unfortunately, they suffer from an important limitation: they only simulate a single interaction between the ray of

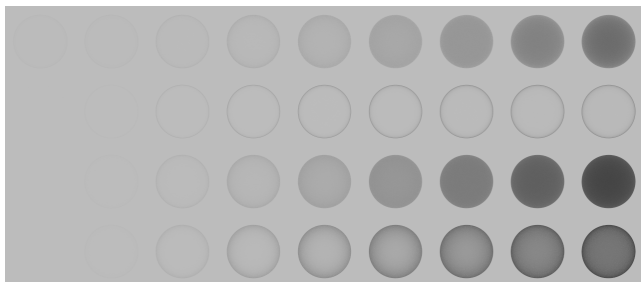


Figure 2: Furnace test on a set of spheres made of different materials with a roughness value that increases from left to right. From top to bottom: metal, plastic, thin glass and thick glass.

light and the surface. What should happen, in reality, is that the ray of light should be scattered several times between different microfacets before being eventually reflected in the viewing direction. As a consequence, the rendered material becomes darker and darker as the value of the roughness increases. This effect is due to the fact that multiple bounces are absent in perfectly smooth surfaces, but become not negligible at high roughness values.

This behaviour becomes clearly visible if we run the furnace test. This test consists in computing a lighting integral against a constant environment light. If we consider a perfectly white material, it should always evaluate to the same color as the background, if there is no energy loss or gain. In the example shown in Figure 2 instead, we can see a substantial amount of energy loss, especially for high roughness values. More formally, the bidirectional reflectance distribution function (BRDF) results to be not energy preserving, because part of the energy is lost while ignoring secondary interactions.

In this work, we face the problem of energy loss in microfacet models. We start analyzing the current state-of-the-art techniques that address this limitation. Correct methods simulate the multiple bounces stochastically [HHdD16; WJF*22], but remain cumbersome to integrate into most renderers, especially on GPUs. Instead, we focus mainly on energy compensation methods [KC17; Tur19] that rescale the BRDF to account for the missing energy. These methods involve the computation of the directional albedo, i.e. the fraction of the incident radiation which is reflected in the viewing direction. This quantity is expressed as an integral which does not have a closed-form solution, so it is necessary to precompute and store it in two or three-dimensional look-up tables.

We developed a set of analytic approximations of the directional albedo to avoid the use of look-up tables to store its values. We provide numerical approximations of the two-dimensional look-up table used for conductors and of the three-dimensional ones used for dielectrics and materials composed of a specular layer on top of a diffuse one, such as plastics, for the microfacet model based on the GGX distribution function.

We found the best compromise between accuracy and number of coefficients in a rational polynomial of degree three both for the 2D and the 3D cases. This results in only 19 coefficients for the approximation of the two-dimensional look-up table and only 39 co-

efficients for the approximation of the three-dimensional ones. Our analytic approximations represent a more practical solution with respect to look-up tables, since they are easier to integrate into an existing rendering architecture, they are more suited for GPU computations and they have a comparable computational cost.

We validate our results both by measuring the fitting error and by running the furnace test. Our tests highlight that materials rendered using our analytic approximations match almost exactly the behaviour of the ones rendered with the use of precomputed look-up tables, resulting in an energy-preserving model even at maximum roughness. Moreover, our final renders show the emergence of expected phenomena, such as the increase in intensity and saturation as the surface gets rougher.

The software we developed to fit our analytic approximations is open-source and publicly available on *GitHub*. It can be easily used to fit other scattering models and can be found at <https://github.com/dsforza96/energy-preservation>.

2. Related Work

In the previous section, we highlighted the energy loss of microfacet models. In the following, we analyze the state-of-the-art techniques that try to address this problem.

Stochastic Models As we already said, the limit of microfacet models is the fact that they simulate only a single interaction between the ray of light and the surface. Heitz et al. [HHdD16] derived a stochastic method that not only simulates the first interaction between the ray of light and the surface but also all the consecutive bounces. It works by modeling the rough material as a volume with the constraint of a sharp interface representing the surface of the object. The BRDF is then evaluated by performing a random walk in the medium. In order to validate their method, they compared their BRDF to the light scattering from a surface made of explicit microfacets, obtained by triangulating it according to the microfacet distribution function. They observed that their model predicted both the albedo and the shape of the multiple scattering BRDF with a high level of precision.

In two concurrent and independent works, Kulla and Conty [KC17] and Turquin [Tur19] highlighted some limitations of the method proposed by Heitz et al. [HHdD16]. Due to its stochastic nature, it needs random numbers to sample and evaluate the BRDF and this makes it difficult to integrate it into an existing rendering architecture. Moreover, for similar reasons, it results to be a computationally very expensive method, with a slowdown in rendering performance which ranges from a factor of 7 up to a factor of 15. Even if the method has been lately improved by Wang et al. [WJF*22] in terms of required number of samples, it is still not suited for real-time applications. On the other hand, we can consider the method by Heitz et al. [HHdD16] a ground-truth solution given its extreme accuracy.

Energy Compensation Methods Energy compensation methods try to compensate for the loss of energy by adding to the BRDF representing the first bounce a term which accounts for all subsequent bounces. Thus, we can see our BRDF $\rho(\omega_o, \omega_i)$ as the sum of

two terms, the first one accounting for the single main interaction and the second one for all the multiple secondary ones:

$$\rho(\omega_o, \omega_i) = \rho_{ss}(\omega_o, \omega_i) + \rho_{ms}(\omega_o, \omega_i) \quad (1)$$

This family of techniques is based on the concept of directional albedo, that is defined as the fraction of the incident radiation which is reflected in a given direction. Due to the law of conservation of energy, it can never be greater than 1. Given a BRDF $\rho(\omega_o, \omega_i)$ and denoting with H the hemisphere and with n the surface normal, the directional albedo $E(\omega_o)$ is given by:

$$E(\omega_o) = \int_H \rho(\omega_o, \omega_i) |n \cdot \omega_i| d\omega_i \quad (2)$$

If we ignore for the moment the absorption due to the Fresnel term, which is equivalent to saying that the material is perfectly white, the following relationship must hold:

$$E(\omega_o) = E_{ss}(\omega_o) + E_{ms}(\omega_o) = 1 \quad (3)$$

The idea behind the method proposed by Kulla and Conty [KC17] is to use a diffuse BRDF to account for all the secondary bounces on the surface. This can be seen as a generalization of a previous work by Kelemen and Szirmay-Kalos [KS01] in which the authors try to address the problem of energy preservation in the specific case of glossy materials. Following the derivation used in the work by Kelemen and Szirmay-Kalos [KS01], they formulate the multiple scattering BRDF as follows:

$$\rho_{ms}(\omega_o, \omega_i) = F_{ms} \frac{(1 - E_{ss}(\omega_o))(1 - E_{ss}(\omega_i))}{\pi(1 - E_{avg})} \quad (4)$$

where F_{ms} is a separate term which accounts for the Fresnel absorption at each secondary bounce and E_{avg} is the average albedo (the average of the directional albedo for all the possible viewing directions) defined as:

$$E_{avg} = \frac{1}{\pi} \int_H E_{ss}(\omega_o) |n \cdot \omega_o| d\omega_o \quad (5)$$

Differently from Kulla and Conty [KC17], Turquin [Tur19] started his work from an observation on the results provided by Heitz et al. [HHdD16]: the secondary BRDFs do not have a diffuse shape, whereas they look like a scaled-down version of the primary one. This observation led the author to formulate the multiple scattering BRDF as the primary BRDF multiplied by a scaling factor $k_{ms}(\omega_o)$ which depends on the viewing direction:

$$\rho_{ms}(\omega_o, \omega_i) = F_{ms} k_{ms}(\omega_o) \rho_{ss}(\omega_o, \omega_i) \quad (6)$$

If we ignore for the moment the effect of Fresnel absorption on the multiple scattering BRDF, we can consider the BRDF $\rho(\omega_o, \omega_i)$ as a normalized version of the single scattering BRDF $\rho_{ss}(\omega_o, \omega_i)$:

$$\rho(\omega_o, \omega_i) = \frac{\rho_{ss}(\omega_o, \omega_i)}{E_{ss}(\omega_o)} \quad (7)$$

The BRDF defined this way is energy preserving by construction since it verifies Equation 3:

$$E(\omega_o) = \int_H \frac{\rho_{ss}(\omega_o, \omega_i)}{E_{ss}(\omega_o)} |n \cdot \omega_i| d\omega_i = \frac{E_{ss}(\omega_o)}{E_{ss}(\omega_o)} = 1 \quad (8)$$

Given this observation, the author derives the scaling factor

$k_{ms}(\omega_o)$, which in its final form is defined as follows:

$$k_{ms}(\omega_o) = \frac{1 - E_{ss}(\omega_o)}{E_{ss}(\omega_o)} \quad (9)$$

For what concerns the F_{ms} term, which accounts for the Fresnel absorption at each secondary bounce, Turquin [Tur19] explored different possibilities, coming to the conclusion that F_0 , i.e. the color at normal incidence, is a very simple yet good enough approximation.

Both methods illustrated so far involve the computation of the direction albedo $E_{ss}(\omega_o)$. Unfortunately, there is no closed-form solution for it, but it is smooth enough to be precomputed and stored in a look-up table of a reasonable size. The result is a 2D look-up table, storing values for the albedo varying the roughness and the viewing direction. Under the assumption of an azimuthal invariant BRDF, the outgoing direction can be represented using one single angle, which is the angle between the viewing direction and the surface normal. Turquin [Tur19] suggests parametrizing the table with the square root of the roughness and the cosine of this angle. With the use of look-up tables defined this way, both methods achieve similar and state-of-the-art results. The same observation is also valid for the average albedo employed in the method by Kulla and Conty [KC17], but, of course, in this case a 1D look-up table is needed.

Analytic Approximations As an alternative to the use of look-up tables, Kulla and Conty [KC17] derived a numerical fit of the directional albedo. However, they do not consider it as precise as the use of the tables themselves and discourage its use. More recently, a different analytic approximation has been developed in the *MaterialX Physically Based Shading* system [Aca21]. It ensures results comparable to the one with the use of precomputed tables, but it is limited to the case of conductive materials. In our work, we also deal with glossy materials and dielectrics, providing a more general framework to compensate for the loss of energy in different scenarios.

3. Energy compensation

In the next sections, we will analyze the different classes of materials we worked on. We decided to work with the GGX distribution function [WMLT07] that nowadays is considered the industry standard both in physically-based and real-time rendering.

3.1. Conductors

The first class of materials we addressed is conductors, which are materials that conduct electricity. This fundamental characteristic influences the way how light interacts with metals like steel and gold. When light hits a surface made of this kind of material, it can be reflected or absorbed, but it can never pass through the surface itself.

Both methods by Kulla and Conty [KC17] and Turquin [Tur19] involve the precomputation of the directional albedo $E(\omega_o)$ of the single scattering BRDF. We have already introduced its definition in Equation 2. The variable of integration, the incoming direction ω_i , varies across the hemispherical domain H . We can express this

variable into a spherical coordinates system using two angles: a polar angle θ_i , ranging from 0 to $\frac{\pi}{2}$, and an azimuthal angle ϕ_i , ranging from 0 to 2π . If we write the incoming direction, together with the outgoing direction ω_o , in this coordinate system, Equation 2 becomes a double integral of the form:

$$E(\theta_o, \phi_o) = \int_0^{2\pi} \int_0^{\frac{\pi}{2}} \rho(\theta_o, \phi_o, \theta_i, \phi_i) |\cos \theta_i| \sin \theta_i d\theta_i d\phi_i \quad (10)$$

Assuming a BRDF invariant to rotations along the surface normal, we can set $\phi_o = 0$ and substitute ϕ_o and ϕ_i with their difference $\phi = \phi_i - \phi_o$. We obtain:

$$E(\theta_o) = \int_0^{2\pi} \int_0^{\frac{\pi}{2}} \rho(\theta_o, \theta_i, \phi) |\cos \theta_i| \sin \theta_i d\theta_i d\phi \quad (11)$$

By reparameterization, we can substitute the polar angles θ with their cosine $\mu = \cos \theta$. After the appropriate change of variable $d\mu_i = -\sin \theta_i d\theta_i$, we get the final form:

$$E(\mu_o) = \int_0^{2\pi} \int_0^1 \rho(\mu_o, \mu_i, \phi) |\mu_i| d\mu_i d\phi \quad (12)$$

We choose to follow the derivation of the multiple scattering term for conductors provided by Turquin [Tur19] because it is better motivated with respect to the one by Kulla and Conty [KC17]. Remembering that F_0 is the color at normal incidence, we define it as:

$$\rho_{ms}(\omega_o, \omega_i) = F_0 \frac{1 - E_{ss}(\omega_o)}{E_{ss}(\omega_o)} \rho_{ss}(\omega_o, \omega_i) \quad (13)$$

The equation for the directional albedo, given that $\rho_{ss}^*(\mu_o, \mu_i, \phi)$ is the BRDF without the Fresnel term, becomes:

$$E_{ss}(\mu_o) = \int_0^{2\pi} \int_0^1 \rho_{ss}^*(\mu_o, \mu_i, \phi) |\mu_i| d\mu_i d\phi \quad (14)$$

In particular, we remember that the single-scattering microfacet BRDF for reflection, ignoring Fresnel absorption and denoting with h the halfway vector between the incoming and outgoing directions, with $D(h)$ the microfacet normal distribution function and with $G(\omega_o, \omega_i)$ the bidirectional shadowing-masking function, is defined as follows:

$$\rho_{ss}^*(\omega_o, \omega_i) = \frac{D(h)G(\omega_o, \omega_i)}{4|n \cdot \omega_o||n \cdot \omega_i|} \quad (15)$$

3.2. Glossy materials

The second class of materials we examined are glossy materials, such as plastics. Nowadays, to obtain their characteristic appearance, they are modeled by overlapping a specular white BRDF onto a diffuse colored one. However, naively summing a microfacet BRDF with a diffuse one is not energy preserving. In fact, we have to consider that the energy which is reflected away from the specular layer cannot reach the underlying diffuse one. As a result, we get extra energy at grazing angles, where the Fresnel term is near 1, especially at low roughness. The diffuse term must be modulated proportionally to the energy which remains after the interaction with the specular layer. A coarse approximation of this amount of energy is represented by the Fresnel term $F(\omega_o)$. Denoting with $\rho_{diff}(\omega_o, \omega_i)$ the diffuse BRDF, our model can be written

as follows:

$$\rho(\omega_o, \omega_i) = \rho_{ss}(\omega_o, \omega_i) + (1 - F(\omega_o))\rho_{diff}(\omega_o, \omega_i) \quad (16)$$

The Fresnel term is an overestimation of the energy which remains after the interaction with the specular layer, because it represents the amount of energy that would be reflected away by a perfectly smooth surface. To face this limitation, Kulla and Conty [KC17] scaled down the diffuse term proportionally to the directional albedo of the specular BRDF layer, accounting for multiple bounces too.

Differently from conductors, the look-up table storing the values of the directional albedo must include also the Fresnel term, because it influences the fraction of energy that is transmitted by the specular layer. As a consequence, we need a three-dimensional look-up table with a further dimension representing the index of refraction, on which the Fresnel term depends. Turquin [Tur19] suggests parametrizing it by the reflectivity at normal incidence F_0 , ranging from 0 to 1, instead of using directly the index of refraction itself. The directional albedo of the specular layer is given by:

$$E_{spec}(\mu_o) = \int_0^{2\pi} \int_0^1 \frac{\rho_{ss}(\mu_o, \mu_i, \phi)}{E_{ss}(\mu_o)} |\mu_i| d\mu_i d\phi \quad (17)$$

Thus, our new energy-preserving BRDF becomes:

$$\rho(\omega_o, \omega_i) = \frac{\rho_{ss}(\omega_o, \omega_i)}{E_{ss}(\omega_o)} + (1 - E_{spec}(\omega_o))\rho_{diff}(\omega_o, \omega_i) \quad (18)$$

3.3. Dielectrics

The last class of materials we worked on is dielectrics, i.e. materials that do not conduct electricity. This characteristic translates to the fact that light cannot only be reflected or absorbed, but it can also continue its path through the surface. The BRDF becomes a bidirectional scattering distribution function (BSDF), which is the sum of a BRDF and a bidirectional transmittance distribution function (BTDF). Turquin [Tur19] observed that for transparent and translucent materials, such as glass and ice, in order to obtain an energy-preserving BSDF, what can be normalized is the sum of the reflected and transmitted energies. Thus, being $\rho_{ss}^R(\omega_o, \omega_i)$ the single scattering BRDF, $\rho_{ss}^T(\omega_o, \omega_i)$ the single scattering BTDF, we have:

$$\rho(\omega_o, \omega_i) = \frac{\rho_{ss}^R(\omega_o, \omega_i) + \rho_{ss}^T(\omega_o, \omega_i)}{E_{ss}(\omega_o)} \quad (19)$$

Since we are dealing with a BSDF that also involves transmission, the directional albedo must be computed integrating over the whole sphere. However, we preferred to compute two separate integrals, one for the BRDF and one for the BTDF, in order to avoid the discontinuity at $\mu_i = 0$, resulting in a more stable computation. The directional albedo of the reflection lobe is similar to one of conductors, but includes the Fresnel term and is given by:

$$E_{ss}^R(\mu_o) = \int_0^{2\pi} \int_0^1 \rho_{ss}^R(\mu_o, \mu_i, \phi) |\mu_i| d\mu_i d\phi \quad (20)$$

The directional albedo of the transmission lobe, instead, is inte-

grated with the cosine μ_i ranging from -1 to 0 :

$$E_{ss}^T(\mu_o) = \int_0^{2\pi} \int_{-1}^0 \rho_{ss}^T(\mu_o, \mu_i, \phi) |\mu_i| d\mu_i d\phi \quad (21)$$

Finally, the total directional albedo, characterizing the whole BSDF, is:

$$E_{ss}(\mu_o) = E_{ss}^R(\mu_o) + E_{ss}^T(\mu_o) \quad (22)$$

Also in this case, we have to include the Fresnel term in the computation (and, as a consequence, use a 3D look-up table), because it determines the ratio between the reflected and transmitted energies. Moreover, it is necessary to store two tables: the first one is used when the ray of light travels from air toward the material, while the second one for the opposite direction, remembering to invert the index of refraction of the medium in the latter situation.

The BRDF is equal to the one for conductors, but including the Fresnel term $F(\omega_o)$, while the transmission part, denoting with $\eta = \frac{n_i}{n_o}$ the relative index of refraction, is:

$$\rho_{ss}^T(\omega_o, \omega_i) = \frac{|\omega_i \cdot h| |\omega_o \cdot h| (1 - F(\omega_o)) D(h) G(\omega_o, \omega_i)}{|\omega_i \cdot n| |\omega_o \cdot n| (\eta(\omega_i \cdot h) + (\omega_o \cdot h))^2} \quad (23)$$

3.4. Thin Dielectrics

Besides proper dielectrics, we worked also on a simplification of them, which we denote as thin dielectrics. They are an approximation of real dielectrics which do not simulate refraction. This model is useful in rendering systems because the majority of transparent objects we are familiar with, such as windows, are thin enough so that the rays of light are not bent in a significant manner when they pass through them.

The approximation results in two identical shapes for the BRDF and the BTDF and thus there is no need for the third dimension accounting for the ratio between reflected and transmitted energies in the look-up table. Furthermore, given that the transmission lobe is an upside-down version of the reflection one, the sum of their directional albedo can be computed as defined in Equation 14. Thus, we can exploit the same look-up table computed for conductive materials.

3.5. Analytic Approximation

In the last sections, we have seen that energy compensation methods involve the precomputation of the directional albedo which needs to be stored in small tables. The main goal of this work is to avoid the use of these look-up tables, trying to develop a set of analytic approximations of the directional albedo of conductive, glossy and dielectric materials.

Given the smoothness that characterizes the directional albedo, we individuated in polynomials a good class of functions to try to approximate it. Moreover, the fact that polynomial regression can be solved in closed form strengthened our choice. Unfortunately, polynomials did not ensure us the performance we expected using a reasonable number of coefficients. Thus, we decided to extend our set of candidate functions to rational polynomials. We tried to approximate high-resolution versions of the look-up tables, computed as described in the previous section, using polynomials and

rational functions up to degree 10 for the two-dimensional case and polynomials up to degree 7 and rational functions up to degree 5 for the three-dimensional one.

In the case of conductors, we maintained the parametrization proposed by Turquin [Tur19], varying the cosine of the angle between the outgoing direction and the surface normal, along the first dimension, and the square root of the roughness, along the second dimension. Both quantities range from 0 to 1. For the third dimension, needed in the case of glossy materials and dielectrics, the author suggests using the reflectivity at normal incidence F_0 instead of the index of refraction directly. Similarly to what Kulla and Conty did in their work [KC17], for dielectrics we tabulated the directional albedo for values of the index of refraction which go from 1 to 3 (or, more precisely, for the corresponding values of F_0 which go from 0.0125 to 0.25).

4. Results

In this section, we describe our experimental setup and present our results. We also explain how we validated our method and finally report some renders to carry out a qualitative evaluation.

We solved the directional albedo integral using the method of the numerical quadrature. In particular, we wrote our code in *Python* and exploited the *SciPy* library [VGO*20]. In order to obtain a more accurate numerical fit, we computed a higher-resolution version of the 32×32 and $32 \times 32 \times 32$ look-up tables suggested by Turquin [Tur19]: 1024×1024 for the two-dimensional table and $128 \times 128 \times 128$ for the three-dimensional ones.

To fit the rational polynomials, we exploited the API for curve fitting which implements an extension of the *Trust Region Reflective* algorithm [BCL99]. The mean absolute error for each fit is reported in Figure 3. We found the rational polynomial of degree three to be the best compromise between accuracy and number of coefficients, resulting in only 19 coefficients for the approximation of the two-dimensional look-up table and only 39 coefficients for the approximation of the three-dimensional ones. Obviously, we could achieve better accuracy choosing functions of a higher degree, but at the cost of a fast growth in terms of number of coefficients. The numerical fits we found for each class of materials are reported in Appendix A.

We based the validation of our method on the furnace test. We run the furnace test writing a custom shader for the *Yocto/GL* rendering system [PNC19]. Figure 4 shows the results of the furnace test for all kinds of material we worked on. As we can notice, they highlight that materials rendered using our analytic approximations match almost exactly the behaviour of the ones rendered with the use of precomputed look-up tables, resulting in an energy-preserving model even at maximum roughness. However, in the particular case of dielectrics, we could not achieve a perfectly energy-preserving result for values of the index of refraction near the boundary of the interval we chose to fit, i.e. 1 and 3. This is probably due to the difficulty of polynomials to adapt to the behaviour of the BSDF in presence of total internal reflection, which translates to a non-smooth shape of the directional albedo. In future work, we plan to explore the possibility to fit better the albedo of dielectrics moving to a different class of functions.

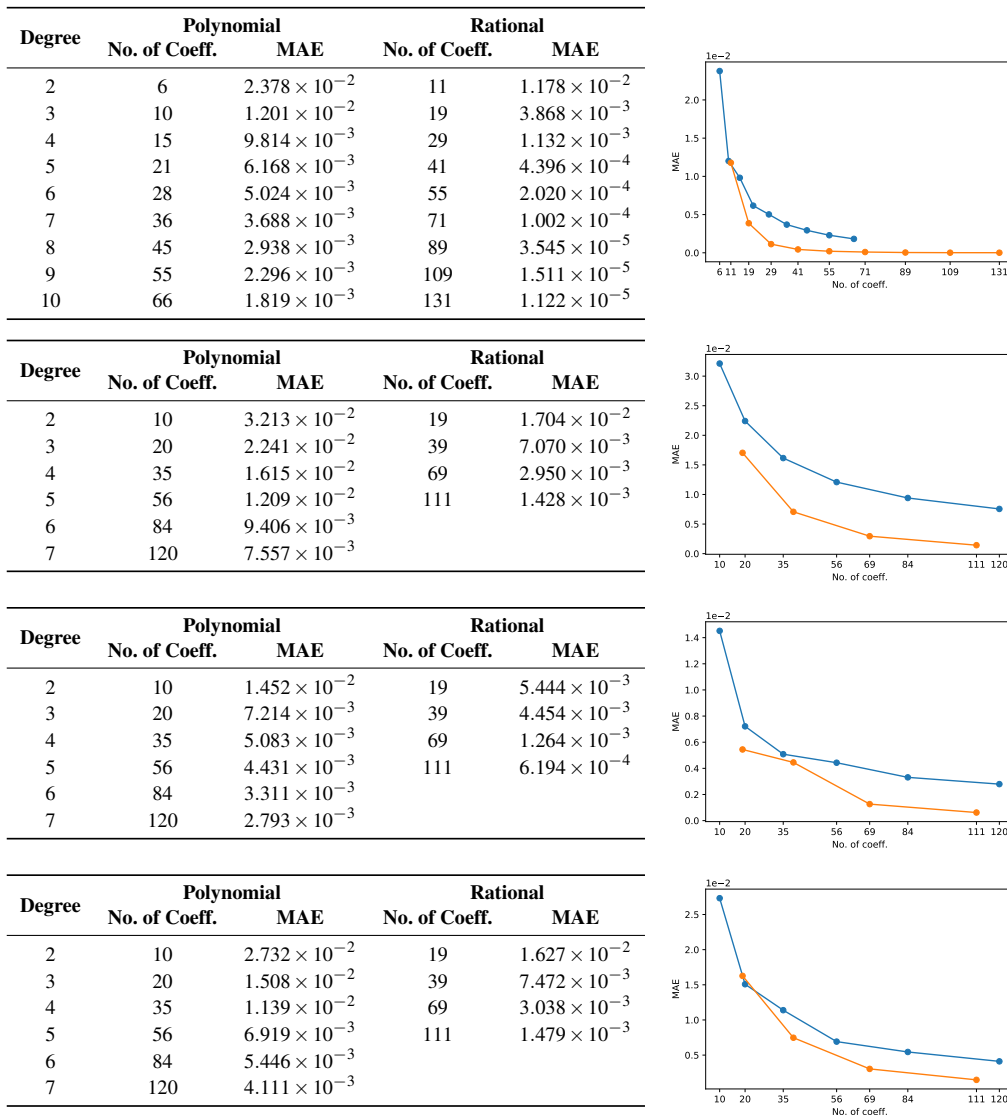


Figure 3: Left: Number of coefficients and mean absolute error (MAE) of the numerical fits of the directional albedo of, from the top, conductors, glossy materials, dielectrics and dielectrics with inverted index of refraction. Right: MAE of the same numerical fits against number of coefficients of polynomials (blue curve) and rational functions (orange curve).

Finally, we performed a qualitative analysis by rendering golden, plastic and glass spheres (Figure 5) together with the rendering of a more complex model made of the same set of materials (Figure 1). The effect of energy compensation is quite noticeable for conductors and glossy materials and becomes even more evident in the case of dielectrics. Moreover, they show the emergence of expected phenomena, such as the increase in intensity and saturation as the surface gets rougher.

5. Conclusions and Future Work

In this work, we addressed the problem of energy loss in microfacet models. We decided to follow an energy-compensation approach and developed a set of analytic approximations of the directional

albedo to obviate the need of look-up tables to store its values. We provide numerical approximations for the GGX distribution function for conductors, dielectrics and materials composed of a specular layer on top of a diffuse one, such as plastics.

In future work, we plan to improve the energy compensation in the case of dielectrics, which still lose energy if we vary the index of refraction far from the canonical value of 1.5. Linearly transformed cosines [HDHN16; KHDN22] represent a promising class of functions to fit the behaviour of the BSDF and have been applied successfully to the domain of realistic cloth appearance modeling [ZBC22]. In our scenario, we think they could be a valid alternative to the use of rational polynomials.

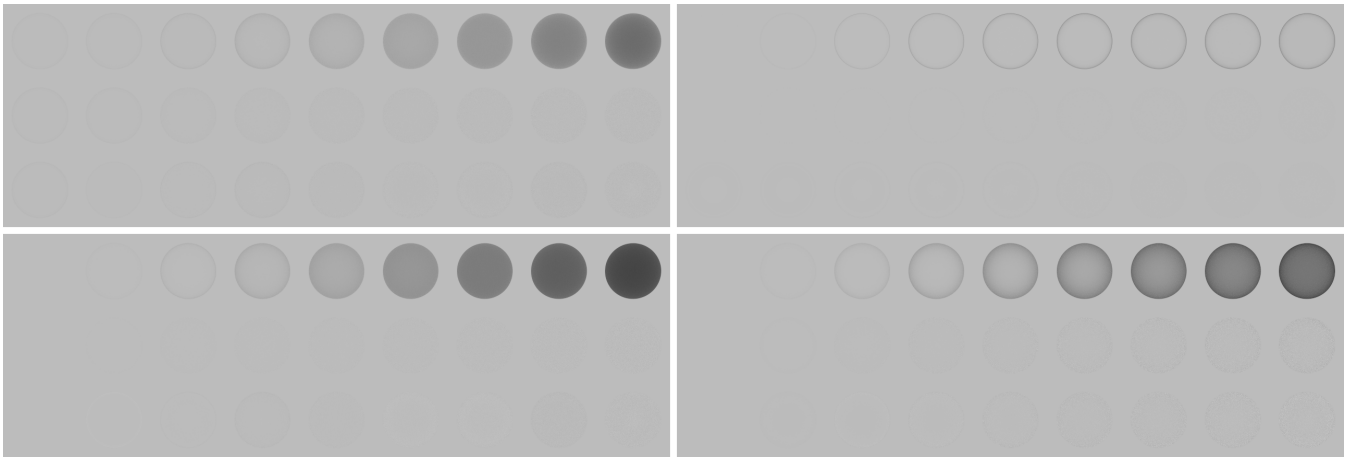


Figure 4: Furnace test for conductors (top left), glossy materials (top right), thin dielectrics (bottom left) and proper dielectrics (bottom right). Top row: no energy compensation. Middle row: energy compensation with the use of look-up tables. Bottom row: energy compensation with the use of our analytic approximations. Roughness increases from left to right.

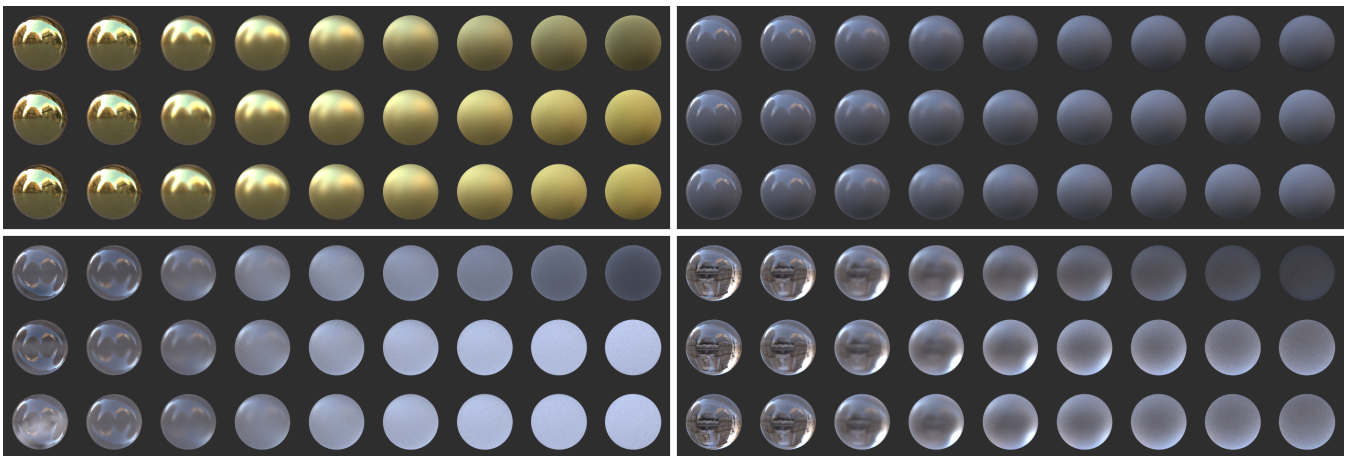


Figure 5: Golden (top left), plastic (top right), thin glass (bottom left) and thick glass (bottom right) spheres with a roughness value that increases from left to right. Top row: no energy compensation. Middle row: energy compensation with the use of look-up tables. Bottom row: energy compensation with the use of our analytic approximations.

Acknowledgements

Dragon model courtesy Stanford Computer Graphics Laboratory [PJH]. Environment map thanks to Andreas Mischok [Mis].

References

- [Aca21] ACADEMY SOFTWARE FOUNDATION. *MaterialX*. 2021. URL: <https://github.com/AcademySoftwareFoundation/MaterialX> 3.
- [BCL99] BRANCH, MARY ANN, COLEMAN, THOMAS F, and LI, YUYING. “A subspace, interior, and conjugate gradient method for large-scale bound-constrained minimization problems”. *SIAM Journal on Scientific Computing* 21.1 (1999), 1–23 5.
- [HDHN16] HEITZ, ERIC, DUPUY, JONATHAN, HILL, STEPHEN, and NEUBELT, DAVID. “Real-time polygonal-light shading with linearly transformed cosines”. *ACM Transactions on Graphics (TOG)* 35 (2016), 1–8 6.
- [HHdD16] HEITZ, ERIC, HANIKA, JOHANNES, D’EON, EUGENE, and DACHSBACHER, CARSTEN. “Multiple-scattering microfacet BSDFs with the Smith model”. *ACM Transactions on Graphics (TOG)* 35.4 (2016), 1–14 2, 3.
- [KC17] KULLA, CHRISTOPHER and CONTY, ALEJANDRO. “Revisiting physically based shading at imageworks”. *SIGGRAPH Course, Physically Based Shading* 2.3 (2017) 2–5.
- [KHDN22] KT, AAKASH, HEITZ, ERIC, DUPUY, JONATHAN, and NARAYANAN, PJ. “Bringing Linearly Transformed Cosines to Anisotropic GGX”. *Proceedings of the ACM on Computer Graphics and Interactive Techniques* 5.1 (2022), 1–18 6.
- [KS01] KELEMEN, CSABA and SZIRMAY-KALOS, LASZLO. “A Microfacet Based Coupled Specular-Matte BRDF Model with Importance Sampling.” *Eurographics (short presentations)*. 2001 3.
- [Mis] MISCHOK, ANDREAS. *Quattro Canti HDRI · Poly Haven*. URL: https://polyhaven.com/a/quattro_canti 7.

- [PJH] PHARR, MATT, JAKOB, WENZEL, and HUMPHREYS, GREG. *Scenes for pbrt-v3*. URL: <https://www.pbrt.org/scenes-v37>.
- [PNC19] PELLACINI, FABIO, NAZZARO, GIACOMO, and CARRA, EDOARDO. “Yocto/GL: A Data-Oriented Library For Physically-Based Graphics”. (2019) 5.
- [TS67] TORRANCE, KENNETH E and SPARROW, EPHRAIM M. “Theory for off-specular reflection from roughened surfaces”. *Josa* 57.9 (1967), 1105–1114 1.
- [Tur19] TURQUIN, EMMANUEL. “Practical multiple scattering compensation for microfacet models”. 45 (2019). URL: https://blog.selfshadow.com/publications/turquin/ms_comp_final.pdf 2–5.
- [VGO*20] VIRTANEN, PAULI, GOMMERS, RALF, OLIPHANT, TRAVIS E, et al. “SciPy 1.0: fundamental algorithms for scientific computing in Python”. *Nature methods* 17.3 (2020), 261–272 5.
- [WJF*22] WANG, BEIBEI, JIN, WENHUA, FAN, JIAHUI, et al. “Position-free multiple-bounce computations for smith microfacet BSDFs”. *ACM Transactions on Graphics (TOG)* 41.4 (2022), 1–14 2.
- [WMLT07] WALTER, BRUCE, MARSCHNER, STEPHEN R, LI, HONG-SONG, and TORRANCE, KENNETH E. “Microfacet Models for Refraction through Rough Surfaces.” *Rendering techniques 2007* (2007), 18th 3.
- [ZBC22] ZELTNER, TIZIAN, BURLEY, BRENT, and CHIANG, MATT JEN-YUAN. “Practical Multiple-Scattering Sheen Using Linearly Transformed Cosines”. *ACM SIGGRAPH 2022 Talks*. 2022, 1–2 6.

Appendix A: Coefficients of the Analytic Approximations

We report here the analytic approximations of the directional albedo that we found to work best. Denoting with r the square root of the roughness ($r = \sqrt{\alpha}$) and given $\mu_o = |\omega_o \cdot n|$, the two-dimensional rational polynomial representing the directional albedo of conductors can be expressed in the form:

$$E(r, \mu_o) = \frac{a_0 + a_1 r + a_2 \mu_o + a_3 r^2 + a_4 r \mu_o + a_5 \mu_o^2 + a_6 r^3 + a_7 r^2 \mu_o + a_8 r \mu_o^2 + a_9 \mu_o^3}{1 + a_{10} r + a_{11} \mu_o + a_{12} r^2 + a_{13} r \mu_o + a_{14} \mu_o^2 + a_{15} r^3 + a_{16} r^2 \mu_o + a_{17} r \mu_o^2 + a_{18} r^3} \quad (24)$$

Similarly, the three-dimensional rational polynomial representing the directional albedo of the other cases, which depend also on the index of refraction parametrized by F_0 , is:

$$E(F_0, r, \mu_o) = \frac{a_0 + a_1 F_0 + a_2 r + a_3 \mu_o + a_4 F_0^2 + a_5 F_0 r + a_6 F_0 \mu_o + a_7 r^2 + a_8 r \mu_o + a_9 \mu_o^2 + a_{10} F_0^3 + a_{11} F_0^2 r + a_{12} F_0^2 \mu_o + a_{13} F_0 r^2 + a_{14} F_0 r \mu_o^2 + a_{15} F_0 \mu_o^2 + a_{16} r^3 + a_{17} r^2 \mu_o + a_{18} r \mu_o^2 + a_{19} \mu_o^3}{1 + a_{20} F_0 + a_{21} r + a_{22} \mu_o + a_{23} F_0^2 + a_{24} F_0 r + a_{25} F_0 \mu_o + a_{26} r^2 + a_{27} r \mu_o + a_{28} \mu_o^2 + a_{29} F_0^3 + a_{30} F_0^2 r + a_{31} F_0^2 \mu_o + a_{32} F_0 r^2 + a_{33} F_0 r \mu_o + a_{34} F_0 \mu_o^2 + a_{35} r^3 + a_{36} r^2 \mu_o + a_{37} r \mu_o^2 + a_{38} \mu_o^3} \quad (25)$$

The coefficients we found for each class of materials are reported in table 1.

Table 1: Coefficients of the rational polynomials approximating the directional albedo of conductors, glossy materials and dielectrics.

	Conductors	Glossy	Dielectrics	Dielectrics (inv. η)
a_0	1.0247	0.043013	0.88205	0.90583
a_1	-10.984	132.98	2.9101	0.66887
a_2	10.918	-0.92736	-0.4865	-0.58909
a_3	46.934	-0.61435	-0.68697	-2.644
a_4	-54.779	-262.23	-2.6111	0.078838
a_5	21.742	-137.75	1.2801	-0.12924
a_6	-30.369	-234.72	-3.0361	-1.3579
a_7	31.919	5.1258	6.01	0.14004
a_8	-8.014	-0.37466	1.5585	1.4653
a_9	-6.2407	9.2847	5.0414	2.3356
a_{10}	-10.218	129.71	0.086795	0.014114
a_{11}	10.955	171.82	1.7978	-0.030981
a_{12}	44.082	400.05	2.4123	-0.093506
a_{13}	-55.335	206.99	3.0965	-0.028034
a_{14}	21.438	1.0848	-13.059	0.20931
a_{15}	-23.745	428.02	6.5016	0.65552
a_{16}	33.265	-2.2109	-5.8326	-0.055329
a_{17}	-7.9269	-6.0564	2.8601	-0.042
a_{18}	-5.931	0.95864	-2.8236	-0.94219
a_{19}		-11.775	-1.999	-0.55064
a_{20}		139.43	2.5766	0.69984
a_{21}		-24.177	-0.88472	-0.25523
a_{22}		-3.7301	-0.2968	-3.2628
a_{23}		-253.78	-1.9874	0.027249
a_{24}		6.7171	7.7758	-0.11726
a_{25}		98.039	11.823	-1.3839
a_{26}		153.19	11.806	0.050796
a_{27}		-184.53	0.77913	0.65825
a_{28}		230.02	8.3709	3.4458
a_{29}		113.94	-0.2142	-0.0099151
a_{30}		66.642	-3.3057	-0.019894
a_{31}		108.32	-7.3967	0.0090828
a_{32}		23.578	26.12	-0.02356
a_{33}		120.04	-38.74	0.16388
a_{34}		102.91	18.953	0.63573
a_{35}		17.03	-7.0976	0.0093054
a_{36}		25.948	0.060185	-0.021682
a_{37}		75.779	-1.6996	-0.43173
a_{38}		49.349	-4.2701	-1.1592